A Kinematic Study of Pulsation in the Dorsal Blood Vessel of the blackworm, *Lumbriculus variegatus*

Kameko Halfmann[1], Kevin Crisp[1]
[1]*Saint Olaf College, Northfield, Minnesota 55057*

The aquatic oligochaete *Lumbriculus variegatus* has a segmented, dorsal blood vessel (DBV) that acts as a peristaltic pump to move blood through the animal's closed circulatory system. We conducted a kinematic study using videography and computational modeling as a first step toward understanding the control of DBV pulsation. Results suggested that pulse rates were highest in the posterior segments, while interpulse intervals and intersegmental delays were longest in the midbody segments. Differences in the interpulse interval distributions across regions suggest that some peristaltic waves initiated in the posterior segments do not propagate all the way to the anterior segments. A simple model consisting of a chain of excitable neuromuscular units replicated these kinetics. This model may be useful in future research aimed at understanding the modulatory effect of biogenic amines on peristalsis of the DBV. Moreover, research into the mechanisms of peristalsis of the DBV may lead to insights into disorders of peristalsis in human and veterinary medicine.

Abbreviations: DBV – Dorsal Blood Vessel; BPM – Beats Per Minute; PW – Pulse Wave; VBV – Ventral Blood Vessel; LV – Lateral Vessel; VNC – Ventral Nerve Canal; I – Intestine

Keywords: Annelid; Peristalsis; Circulation; Neural Network

Introduction

Presently, it is not understood how the peristalsis in the DBV in the blackworm, *Lumbriculus variegatus* (Müller, 1774), is generated or how the rate of pulsation is controlled. From a comparative perspective, molluscan hearts are myogenic, but they are also innervated by nerves that can accelerate or slow the heart rate (Koester et al., 1973). Crustaceans, such as *Limulus*, have neurogenic hearts in which central pattern generators control a myocardium that need not be electrically excitable (Parnas et al., 1969). More closely related to *L. variegatus,* the leech has two longitudinal heart tubes, which have a slow myogenic rhythm that is entrained by cholinergic motor neurons under the control of a single central pattern generator in the anterior segments of the nerve cord (Stent et al., 1979; Calabrese and Peterson, 1983; Calabrese and Maranto, 1986).

The small size and poor accessibility of the nervous system in the blackworm are barriers to elucidating the control of peristalsis; however, the transparent cuticle, the large size of the dorsal blood vessel (DBV) and the red-pigmented blood allow for non-invasive methods of observation that can yield indirect evidence to help explain these mechanisms (see Fig. 1). Moreover, the visibility of the DBV is unique and adds an interesting comparative perspective to similar studies of peristalsis in related species as it allows for direct observation of pulsation. Structurally, *L. variegatus* has a closed circulatory system with a single, continuous longitudinal DBV, likely composed of oblique striated muscles (Wenning et al., 2004; Fig. 1). The DBV lies just beneath the dorsal body wall where it is closely associated with the surface of the body. This is particularly the case in the most posterior 30 segments where body wall muscle is sparse; hence, this
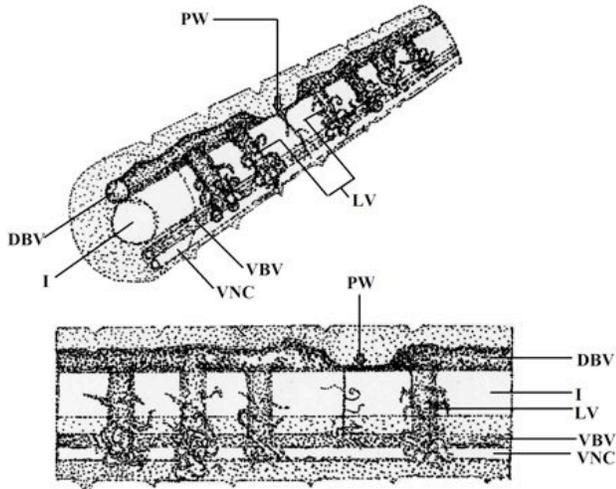
Figure 1: Stipple drawings detailing the *Lumbriculus variegatus* circulatory system. Note the large size of the dorsal blood vessel (DBV), the visibility of the pulse wave (PW), and the poor accessibility to the ventral nerve canal (VNC). Also note the ventral blood vessel (VBV), lateral vessels (LV) and the intestine (I).

region is well adapted for gas exchange in an organism that spends most of its time burrowed in the mud with only its tail exposed (Zoran and Martinez, 2009).

As in other annelids, blood flow depends in part on body wall and gut muscle movement (Beesley et al., 2000), but the DBV of *L. variegatus* also exhibits rhythmic peristalsis (Lesiuk and Drewes, 1999a). These waves pump blood unidirectionally anteriorly, presumably due to the presence of one-way valves (Solc, 2007), with multiple waves visible simultaneously at different locations along the DBV (Lesiuk and Drewes, 1999a). In the anterior portion of the worm, blood flow reverses direction and flows passively through the ventral vessels posteriorly (Lesiuk and Drewes, 1999a). As in the earthworm *Lumbricus terrestris*, *L. variegatus* also has several "hearts" (lateral commissural vessels) that connect with the ventral vessel in some of the anterior segments (Stephenson, 1930), but their rate of contraction may not be coordinated with the activity of the DBV (Prosser et al., 1950).

Here, we present a kinematic study of peristalsis in the DBV using videography, pulse rate variance analyses, and computer simulation to better understand the mechanisms underlying

peristalsis in the blackworm. The model was developed based on observations in order to suggest a mechanism sufficient for the control of peristalsis in the blackworm.

Interestingly, previous data suggests pulse rates as high as 30 BPM in the tip of the tail and as low as 10 BPM in the midbody segments (Lesiuk and Drewes, 1999a). The difference in contraction rates may be due to one pacemaker driving the peristaltic waves throughout the worm, entraining passive followers to contract. Every so often, an excitatory signal could arrive at a follower mechanism and fail to bring that segment to threshold and contract; in which case, the wave would stop, leading to the difference in contraction rates between the posterior and middle. However, this seems unlikely, as the blackworm is autonomous.

Alternatively, pulsation could be controlled by distributed, segmentally reiterated mechanisms. Rhythmic timing elements could be distributed throughout the animal in three possible ways. A reflex could act as a distributed mechanism for coordinating contraction between segments, where distension reflexively triggers contraction. This seems unlikely due to the variability in both the beat-to-beat latency and in the amount of distension from segment to segment. A second distributed mechanism is rhythmic smooth muscle units that are coordinated through gap junctions. This is also unlikely because of the unidirectionality of the peristaltic waves, the abundance of skeletal muscle in other annelid hearts, and the ubiquitous coordination of peristalsis by neural elements across animal species.

Instead, we hypothesize that a feed-forward system of distributed, coupled neuronal oscillators is a sufficient model to explain the control of pulsation in the blackworm, *L. variegatus*. This model is evolutionarily adaptive for this species, which is known to autotomize. Observationally, we aim to replicate the Lesuik and Drewes (1999a) finding, demonstrating differences in pulsation rate between posterior, midbody, and anterior regions of the worm. We hypothesize that we will further see differences in cyclic dynamics of pulsation (such as duty cycle, interbeat interval, and intersegmental delay) between posterior,

midbody, and anterior segments of the worm.

Research into the mechanisms of peristalsis of the DBV may lead to insights into disorders of peristalsis in human and veterinary medicine. Further research could utilize the model as an initial means of testing hypotheses of the effect of pharmacological agents on peristalsis in the blackworm; and more interestingly, the model could be manipulated to replicate peristalsis in the human or nonhuman animal gut and in order to test such hypotheses.

Material and Methods

For observations of the DBV, individual worms were transferred to a slide with a layer of paper towel in a small volume of artificial salt water (ASW) and lightly compressed beneath a cover slip to restrain movement. We avoided more aggressive attempts to immobilize the worms, which are prone to autotomy (Lesiuk and Drewes, 1999b). Pulsations in the DBV became uncoordinated after prolonged handling in this fashion (due to dry environment which led to slowing pulse rate and ectopic beats; data not shown), therefore, we restricted our observations to the first two minutes of mounting on the slide, and worms were discarded after observation. To obtain reliable measurements, we used a zoom stereo dissecting microscope with a 0.8x objective with a 0.7-11.5 zoom; thus the total magnification range used was 0.56x to 9.2x.

Videography

Time lapse images were obtained of live worms using an Olympus SZX16 dissecting microscope (Olympus Imaging America, Center Valley, PA, USA) with a mounted Olympus DP71 video camera. Videos were digitized at a sampling rate of 15 Hz using DP Controller version 3.2.1.276 (Olympus). ImageJ (v. 1.42q, National Institute of Health, Bethesda, MD, USA) was used to extract individual frames and obtain measurements of the diameter of the DBV in consecutive segments. The diameter of the DBV was determined using the straight-line selection tool in ImageJ to measure a line

bisecting the middle of a single segment in the DBV (see Fig. 2a).

Pulse Rate Variability

For pulse rate variability analysis, pulse times were recorded by manually triggering a square pulse generator and digitizing the output of the generator using a Digidata 1322A in
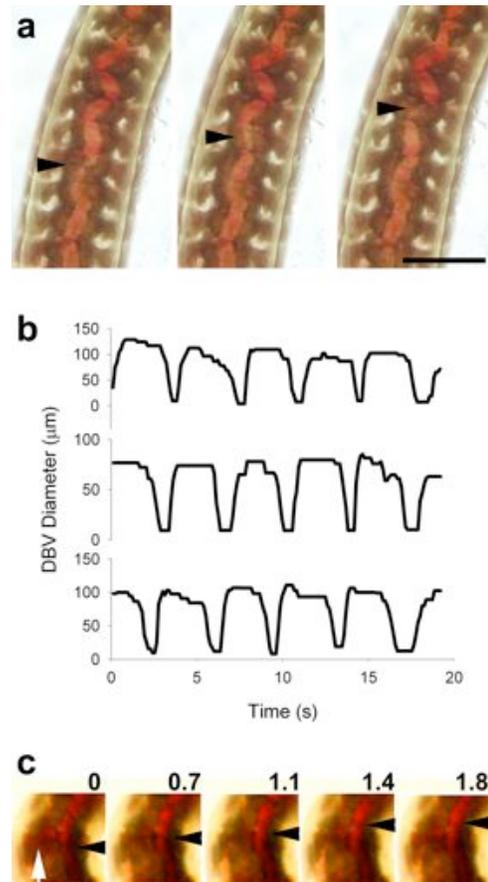

Figure 2: **A:** Time series showing peristaltic pulse traveling anteriorly (toward the top) through the dorsal blood vessel (DBV) in a middle region of the *L. variegatus.* The approximate middle of a pulse is indicated by a black arrowhead in each successive frame. Elapsed time between frames is approximately 0.68 s. Scale bar: 0.5 mm. **B:** Diameter of the DBV as a function of time, measured from three consecutive midbody segments. Contractions propagate from the posterior segments (bottom trace) anteriorly (top trace). Vertical scale bar: 20 µm; horizontal scale bar: 1 s. **C:** Time series demonstrating the segmentally-reiterated lateral vessels that form perpendicular branches from DBV. These vessels also undergo rhythmic contractions that occur at approximately the same time of the DBV contraction passes the junction between the two lateral vessels.

conjunction with the Axoscope software (version 10.2.0.10; MDS Analytical Technologies, Sunnyvale, CA). Inter-pulse intervals were calculated using BioPac software (v. 3.7.1, Goleta, CA). The pulse rate variability analysis was conducted using Kubios HRV (v. 2.0, Biosignal Analysis and Medical Imaging Group, University of Kuopio, Finland), but all graphs in the figures that follow were prepared using SigmaPlot (version 9.01; Systat Software, Inc; Chicago, IL). Statistics are reported as the mean ± standard error (n = number of observations, unless otherwise noted).

Statistical Analyses

Analyses were done in IBM SPSS Statistics (version 19, IBM Co., Somers, NY), unless otherwise specified. Cyclic statistics were analyzed using nonparametric ANOVAs (independent samples Kruskal-Wallis Tests) due to differences in variance across regions.

Computer Modeling

A simple feed-forward neural network model was constructed in Python (www.python.org) using a segmentally-reiterated neuron-like unit (Izhikevich, 2003) that drove an aphysiological isotonic neuromuscular transform (Brezina et al., 2000). The model was derived from observations of wave propagation velocity and wave cycle period. Each unit in the model is driven by two inputs, an intersegmental synaptic input (I_{IS}) from the previous unit (except in the case of the initial unit), and a segmental driving current (I_{SD}) that promotes periodic depolarization and bursting of each unit. These inputs were selected to make the model's peristalsis mimic the observed peristalsis seen in the real worms. From the posterior-most segment, the magnitude of the I_{IS} current decreases at a rate of approximately 3.5% per segment until the midpoint of the model, at which point it increases at the same rate until it reaches its initial level at the most anterior unit. The magnitude of the I_{SD} current decreases steadily at a rate of 2% per unit, such that its maximum level is in the most posterior unit and its minimum is in the most anterior unit.

The membrane potential (*v*) of each unit was described as

$$\dot{v} = 0.04v^2 + 5v + 140 - u + I_{SD} + I_{IS} \quad (1)$$

where *u* is a dimensionless recovery function with kinetics described by

$$\dot{u} = 0.01(0.22v - u) \qquad (2)$$

(Izhikevich, 2003). An impulse was triggered whenever v > 35 mV (impulse threshold), at which point *v* is set to -65 mV and *u* is increased by 3.13. The instantaneous firing rate of a given unit determined muscle contraction of the DBV in the same segment, such that the diameter (*d*) of the DBV at any instant in time is

$$d = 1 - a^3 \qquad (3)$$

where *a* is a simple neuromuscular transform of firing frequency (*f*) into contraction magnitude. The dynamics of the neuromuscular transform are described by

$$\dot{a} = 0.01f(1 - a) - 0.09a \qquad (4)$$

(Brezina et al., 2000). The units are pulse-coupled such that an impulse in unit *n* causes an instantaneous current injection into unit *n*+1 (its anterior neighbor) of magnitude I_{IS}.

The model was analyzed by systematically varying the maximum magnitude (e.g., the magnitude at the most posterior unit) of I_{SD} and I_{IS}. To examine the effect of these currents on cycle period and intersegmental delay, these parameters were normalized on a percent scale such that the period or delay observed at the lowest level of I_{SD} or I_{IS} was 100%. Models were categorized according to emergent behaviors by visual inspection of a 3D animated model (constructed using the VPython module; http://vpython.org/) driven by the neural network and plots of segmental contraction over time (generated using the Matplotlib module http://matplotlib.source forge.net/). The model is available for download through the ModelDB database (http://senselab.med.yale.edu/ ModelDB/default.asp).

Table 1. Differences in cyclic statistics as a function of segment.

	Mean Pulse Rate (BPM)	Intersegmental Delay (s)	Interpulse Interval (s)
Posterior Segments	15.85 ± 2.06 (n = 4)	0.69 ± 0.02 (n = 11)	1.12 ± 0.02 (n = 15)
Midbody Segments	13.74 ± 1.76 (n = 5)	0.91 ± 0.04 (n = 16)	1.66 ± 0.15 (n = 18)
Anterior Segments	13.62 ± 2.33 (n = 4)	0.64 ± 0.04 (n = 12)	1.17 ± 0.21 (n = 16)

Results

Pulses were observed to propagate anteriorly (Fig. 2a) with a mean velocity of 1.26 ± 0.25 segments/s (n = 8). Each pulse was characterized by a transient decrease in the diameter of the DBV in the middle of the segment (Fig. 2b). We did not observe any obvious relationship between peak distension and the onset of the next pulse.

In segments throughout the worm, the DBV also branches into contractile lateral vessels that end blindly and do not connect with the ventral vessel (Lesiuk and Drewes, 1999a). These vessels contract in synchrony with the DBV in midbody segments (Fig. 2c), but may contract less or not at all in anterior segments that also have a lateral commissural "heart" (data not shown). The segmentally-reiterated lateral vessels (Fig. 2c, white arrow) that form perpendicular branches from DBV also undergo rhythmic contractions that occurred at approximately the same time when the DBV

contraction (black arrowheads) passed the junction between the two vessels.

Subtle differences were observed in the properties of the contraction cycle between posterior, midbody and anterior segments of the DBV (Fig. 3). Observationally, it was noted that most beats reached peak diameter immediately following contraction, rarely immediately before. On some beats, peak contraction was maintained throughout the interbeat interval, but more commonly the diameter decreased slightly and then remained at this new diameter until the onset of the next pulse. The mean pulse rate was observed to be slightly lower in anterior segments, as has been previously reported (Lesiuk and Drewes, 1999a), but this difference was not statistically significant. The mean pulse rate was 15.85 ± 2.06 BPM (n = 4) in the posterior segments, 13.74 ± 1.76 BPM (n = 5) in the midbody segments, and 13.62 ± 2.33 BPM (n = 4) in the anterior segments.

Interestingly, the cycle period, intersegmental delay and interpulse interval were longer in the midbody segments than in the posterior segments (Fig. 3; Table 1). Independent samples Kruskal-Wallis Tests revealed significant differences between regions in cycle period ($p < 0.01$) and interbeat interval ($p < 0.05$), but not duty cycle ($p = 0.09$) or intersegmental delay ($p = 0.20$), though both followed a similar pattern.

The difference in the magnitude of the standard error of the interpulse intervals points to a difference in the distribution of interpulse intervals recorded in these three locations. Examination of recordings from individual worm segments reveal a relatively constant

Figure 3: Differences in cyclic statistics as a function of segment. Though the difference between pulse rates observed in anterior and posterior segments was not statistically significant, longer intersegmental delays were observed in the midbody segments. Inter-pulse intervals were longer in the midbody segments, and cycle periods were shortest in the posterior segments, suggesting that peristaltic waves slow down as they pass through the midbody segments.
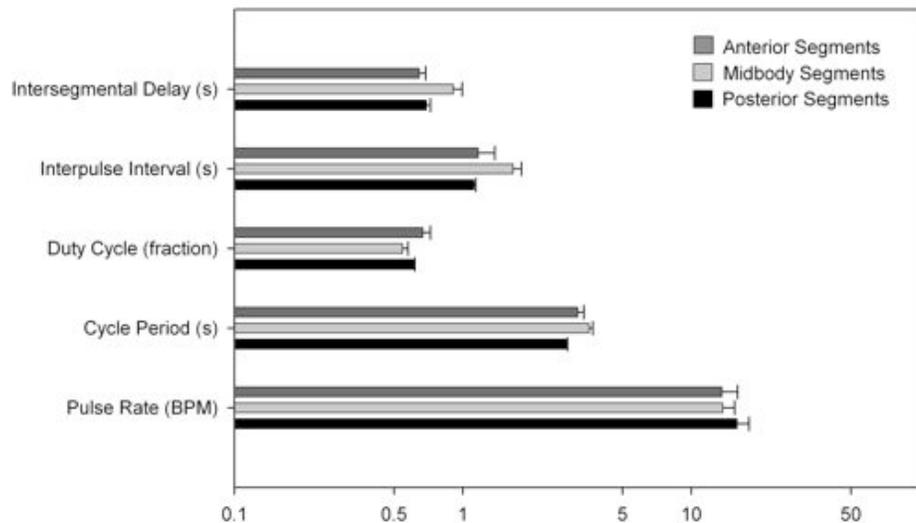
interpulse interval across consecutive pulses in the posterior segments, with increasing variability in interpulse interval anteriorly (Fig. 4a). The corresponding probability densities show that although the average interpulse interval in the midbody segments are longer than the average interpulse interval in the anterior segments, the frequency of very long interpulse intervals (>8 s) is higher toward the anterior segments of the worm (Fig. 4b). Note that these three recordings in Fig. 4a are from three different worms, due to technical limitations, and should not be interpreted as simultaneous activity in three locations of the same worm.

The model of a simple feed-forward chain of excitable integrate-and-fire units demonstrated the observations seen in the animal. In the computational model, I_{IS} and I_{SD} were varied over a broad range of magnitudes, resulting in models with different properties. Models with higher I_{SD} displayed shorter cycle periods (i.e., higher BPM), while models with higher I_{IS} displayed shorter intersegmental delays. For example, when the maximum I_{IS}

was set to 200 (arbitrary units), normalized cycle period (see Methods) decreased exponentially as I_{SD} increased. This decay was well-fit by a two-parameter single exponential decay curve of the form

$$per = 71.25 + 27.88e^{-0.03I_{SD\_max}} \qquad (5)$$

where per is normalized cycle period (adjusted $R^2 = 0.99$; p < 0.005). Similarly, when maximum I_{SD} was held constant at 5 (arbitrary units), normalized intersegmental delay decreased exponentially as maximum I_{IS} increased ($del = 35.94 + 66.95e^{-0.05I_{IS\_max}}$, where del is normalized delay; adjusted $R^2 = 0.97$; p<0.001).

I_{IS} and I_{SD} were also co-varied over a broad range of magnitudes, resulting in the generation of 80 versions of the model. Each model was visually inspected and classified according to the behavior that emerged from the pair of model parameters (Fig. 5). The relationship between these emergent behaviors and the two manipulated parameters was
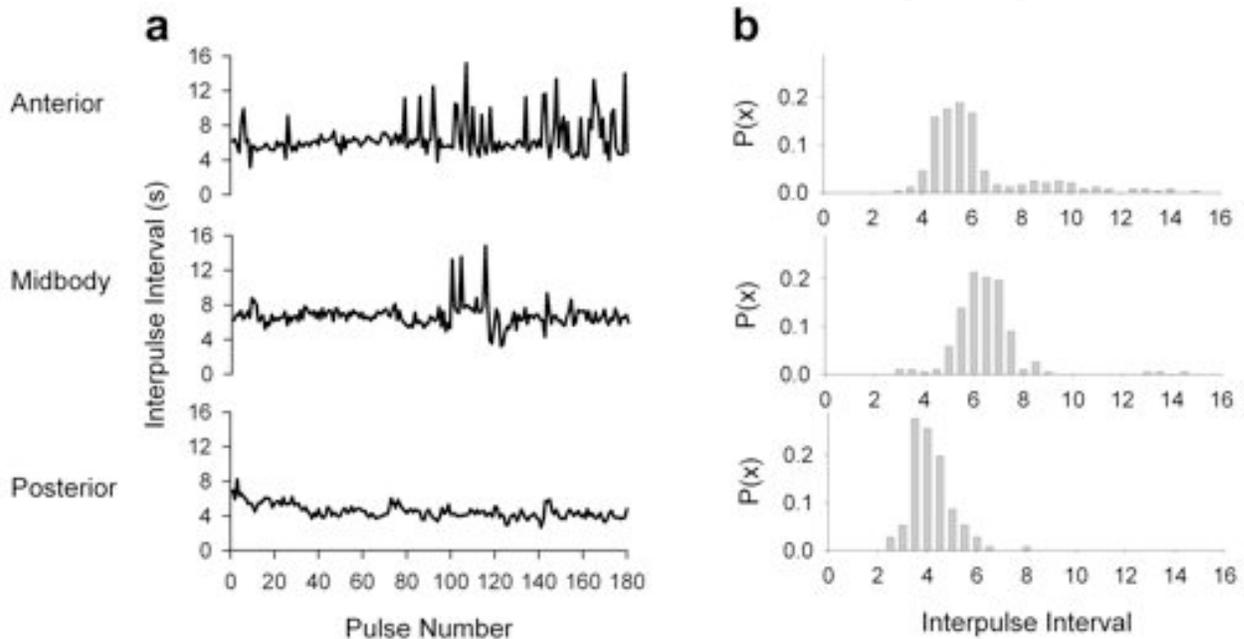

Figure 4: Between-animal differences in interpulse interval variability in more anterior and more posterior segments. **A:** Plot of interpulse interval as a function of pulse number. Interpulse intervals were more variable in the anterior segments of the animal, due to the increasing frequency of long intervals. **B:** Probability densities of interpulse intervals. Although the mean interpulse interval was longest in midbody segments, the increasing frequency of longer intervals toward the anterior segments of the worm is apparent as a skewing of the interpulse interval distribution, especially in the anterior segments.

analyzed by plotting behaviors in two-dimensional parameter space (Fig. 6). Furthermore, at permissive levels of I_{SD}, faithful propagation of waves anteriorly was associated with higher levels of I_{IS}, while lower levels of I_{IS} resulted in failure of peristaltic waves to propagate anteriorly. Interestingly, higher levels of I_{SD} were more frequently associated with models with significant pauses in the midbody segments (Fig. 5c) than with models that showed successful propagation (Fig. 5e), occasional failure (Fig. 5d), or consistent failure (Fig. 5b). The pauses were on occasion so long that the next wave collided with it, resulting in a lower rate of pulsation in the anterior segments than in the posterior segments, although the interpulse intervals appeared to be relatively constant in the anterior segments of these models. Moreover, the pulse rate was lower in anterior segments than in the posterior segments, and the interpulse interval in the anterior

segments showed larger variability than in other models. Significantly, 75% of the models examined produced some peristalsis, and of these 60% developed higher pulse rates in the posterior segments than in the anterior segments due to occasional failure of waves to propagate past the midbody, or slowing down in the midbody segments that resulted in collisions between consecutive peristaltic waves.

Discussion

Presently, it is not well understood how peristalsis in the DBV in the blackworm is generated or how the rate of pulsation is controlled. Previous data suggests pulse rates as high as 30 BPM in the most posterior segments, and as low as 10 BPM in midbody segments (Lesuik and Drewes, 1999b). Here, we used a
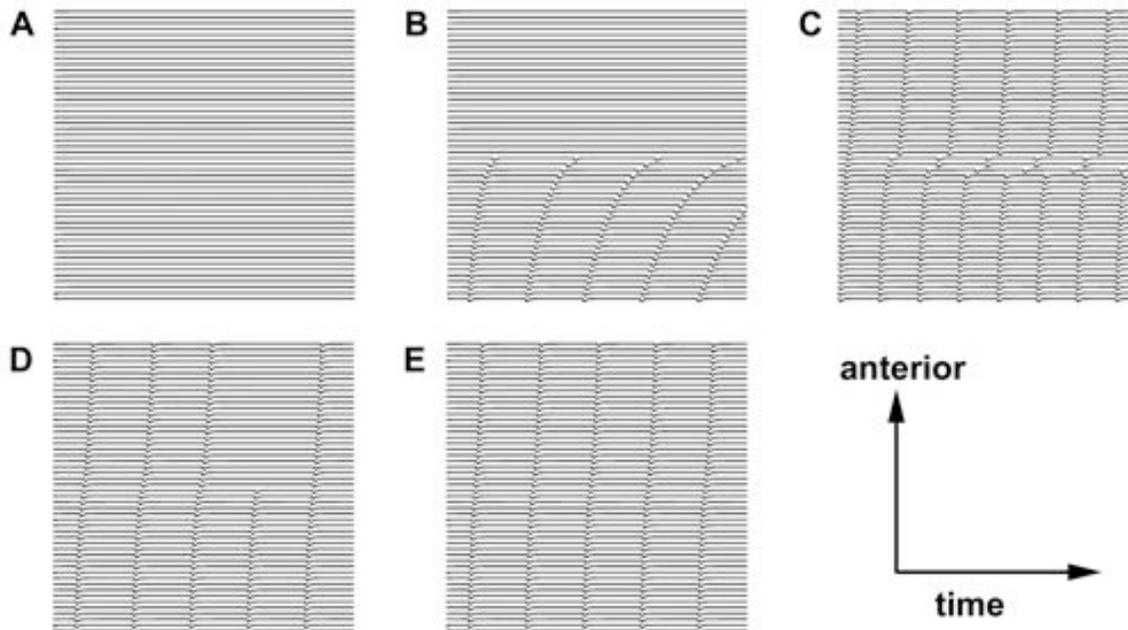

Figure 5: Model behavior changed as the magnitude of the segmental driving current (I_{SD}) and the intersegmental synaptic current (I_{IS}) were co-varied. In panels A-E, each horizontal line represents relative diameter of a single DBV segment; 50 segments are shown, with anterior segments toward the top of each plot. A decrease in diameter is indicated by a downward trajectory. **A:** An example of a quiescent model ($I_{SD} = 1$, $I_{IS} = 200$), showing no contractions in any segment. **B:** A model demonstrating consistent failures of each peristaltic wave ($I_{SD} = 5$, $I_{IS} = 0$), such that no waves progress to the most anterior segments. **C:** A model showing long pauses between contractions in the middle segments ($I_{SD} = 15$, $I_{IS} = 200$), resulting in collisions between some posteriorly-initiated waves and earlier waves that have stalled in the middle. Note that the pulse rate is slower in the anterior than it is in the posterior in these models. **D:** Model showing occasional wave failure in the middle segments ($I_{SD} = 5$, $I_{IS} = 200$). Note that as in **C**, the pulse rate is slower in the anterior than it is in the posterior. **E:** Model showing successful propagation of all waves to the most anterior segments ($I_{SD} = 5$, $I_{IS} = 300$).

kinematic study of peristalsis in the DBV utilizing videography, pulse rate variance analyses and computer simulation to test possible mechanisms to explain our observations. Consistent with Lesuik and Drewes (1999a), our data suggest that pulse rates are highest in the posterior segments, while interpulse intervals and intersegmental delays are longest in the midbody segments. Our choice to analyze statistics across worms, rather than within worms, may explain the smaller magnitude of this difference than in prior observations. Differences in the interpulse interval distributions across regions suggest that some peristaltic waves initiated in the posterior segments do not successfully propagate to the anterior segments. A simple model consisting of a chain of excitable neuromuscular units was sufficient to demonstrate these kinetics. The proposed model suggests two simple mechanisms, intersegmental coupling (I_{IS}) and graded excitatory drive to each unit (I_{SD}), which were derived from the observation that wave propagation velocity and wave cycle period slow down in midbody segments as the waves arrive from their origin in the posterior segments. The model is able to replicate observations, which supports our hypothesis that a system of distributed, coupled neuronal oscillators is a sufficient model to explain the control of pulsation in the blackworm, *L. variegatus*.

One untested hypothesis to explain the above observations is that pulses slow their velocity of propagation and lengthen their cycle period in the midbody segments and sometimes fail to propagate the entire distance to the anterior of the worm. This failure to propagate could occur for two reasons. First, the driving forces that propel the peristaltic wave could be weakest in the midbody segments, and may be insufficiently strong to guarantee that all waves propagate past the midbody segments. In this case, some waves would occasionally fail on their way from the posterior segments to the anterior segments. Second, because pulses are observed to slow their velocity in the midbody segments, the next pulse from the posterior segments may occasionally overtake them. Thus, neural or muscular refractory periods associated with the first peristaltic wave might
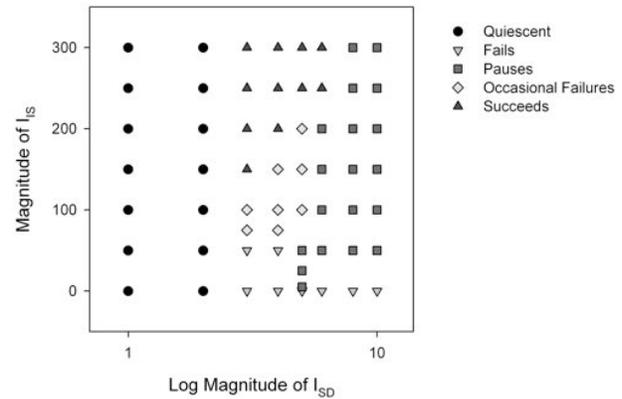

Figure 6: Two dimensional sensitivity analysis showing behaviors that emerge from the model as the magnitude of I_{SD} and I_{IS} are co-varied. Lower levels of I_{SD} resulted in quiescent models, while higher levels resulted in uncoordinated contraction (not shown). Out of the 60 models shown, 8 (13%) demonstrated occasional failure of waves propagating toward the anterior (see Figure 7D), resulting in a lower pulse rate in more anterior segments. 19 models (32%) showed long pauses in the middle, and most of these (83%) demonstrated collisions (see Fig. 4C) within the duration of simulation, which also resulted in a lower pulse rate in the anterior than in the posterior segments.

cause a failure of the second wave to propagate past the midbody segments. In either case, the end result would be a higher mean pulse rate in the posterior segments than in the anterior segments and greater interpulse interval variability in the anterior segments than in the posterior segments.

Like *L. variegatus,* earthworms also show higher pulse rates in the posterior segments than in the anterior segments due to the occasional failure of peristaltic waves (Carlson, 1908). In *L. terrestris*, blood flows anteriorly for the entire length of the DBV, and flows into the DBV in each segment through lateral vessels (Johnston and Johnson, 1902; Johnston, 1903). In contrast, the "hearts," which pump blood out of the DBV toward the ventral vessel, are only found in a subset of anterior segments. Possibly, this pattern of circulation results in higher blood volumes in the middle segments of the worm than in the posterior segments, such that a lower pulse rate in these segments is sufficient to maintain appropriate blood pressure. Furthermore, the additional pressure generation by the anterior hearts may

compensate for a lower pulse rate in the DBV in the anterior segments.

The proposed model suggests simple mechanisms by which peristaltic waves may occasionally fail to propagate. These mechanisms were derived from the observation that wave propagation velocity and wave cycle period slow down in the midbody segments as the waves arrive from their origin in the posterior segments (Fig. 3). If the intensity of the driving excitation to the muscle is relatively lower in amplitude in the midbody segments (than in the posterior segments), the stimulation may not bring the neuromuscular unit to threshold to trigger a contraction, and occasional waves will fail to propagate past the midbody segments. Alternatively, if the wave of excitation traveling anteriorly along the chain of neuromuscular units slows sufficiently in velocity, the units may still be refractory when the next wave arrives, resulting in a collision and failure to propagate further. While leeches have a central motor rhythm underlying their heartbeat, a segmentally distributed system in the blackworm allows for autotomy to occur without largely influencing the livelihood of the animal. Moreover, the abundance of skeletal muscle in other annelid hearts and the ubiquitous coordination of peristalsis by neural elements across animal species make neural oscillators a more evolutionarily fit mechanism of control than distributed rhythmic smooth muscle units coordinated through gap junctions.

On a broader scale, local reflexes play a vital role in controlling peristalsis in the more complex mammalian gastrointestinal tract. Although the proposed model does not take feedback into account, local reflexes may play an important role in regulating pulse rate. Stretch receptors may entrain the rhythm, much as proprioceptors entrain the output of the locust flight pattern generator (Mohl, 1985). If stretch receptors similarly help to entrain the rhythm of the DBV, the relatively larger size of the midbody segments may mean that it takes longer for a segment of the DBV to become sufficiently distended to trigger a contraction. However, we did not observe any correlation between the time at which the DBV relaxed to its maximum diameter and the onset of the next pulse (Fig. 2b). On the other hand, stretch receptors could participate in the regulation of blood pressure in the worm by acting locally to reflexively slow the rate of contraction when pressure rises. A proportionately higher blood volume in the midbody segments might cause a slowing of pulse rate in these segments by such a reflex.

Previous research has indicated that biogenic amines play a role in regulating DBV pulsation in the blackworm (Crisp et al., 2010), supporting a role for neurotransmission in the control of the oligochaete circulatory system. However, little was understood about the neural control of pulsation. The current model can be employed to understand how the biogenic amines are acting to play a role in coordinating stereotypic and adaptive behaviors in invertebrates.

Thus, we conducted a kinematic study using videography, pulse rate variance analyses, and computational modeling as a first step toward understanding the control of DBV pulsation. Results suggested that there are differences in pulse rate and cyclic statistics across regions of the blackworm. Differences in the interpulse interval distributions across regions suggest that some peristaltic waves initiated in the posterior segments do not propagate all the way to the anterior segments. A simple model consisting of a chain of excitable neuromuscular units was created to replicate these observations. This model provides a mechanism sufficient for the control of peristalsis in the blackworm and may be useful in future research aimed at understanding the modulatory effect of biogenic amines on peristalsis of the DBV as well as a first step toward understanding peristalsis in the more complex mammalian gut.

Acknowledgements

acknowledge Caleigh M. Kimberley for her attention to detail and the effort she put into the stipple drawings in Figure 1.

Corresponding Author

Kameko Halfmann
University of Iowa
    3305 Shamrock Dr.
    Iowa City, Iowa 52245
    Kameko-Halfmann@uiowa.edu

References

Beesley PL, Ross GJB, Glasby CJ (2000) Polychaetes & Allies: The Southern Synthesis, Melbourne, Australia: CSIRO Publishing.

Brezina V, Orekhova IV, Weiss KR (2000) The neuromuscular transform: the dynamic, nonlinear link between motor neuron firing patterns and muscle contraction in rhythmic behaviors, J Neurophysiol 83:207-31.

Calabrese RL, Peterson E (1983) Neural control of heartbeat in the leech, Hirudo medicinalis, Symp Soc Exp Biol 37:195-221.

Calabrese RL, Maranto AR (1986) Cholinergic action on the heart of the leech, Hirudo medicinalis, J Exp Biol 125:205-24.

Carlson AJ (1908) Comparative physiology of the invertebrate heart. X. A note on the physiology of the pulsating blood vessels in the worms, Am J of Phys 22:353-56.

Crisp K, Grupe R, Lobsang T, Yang X (2010) Biogenic amines modulate pulse rate in the dorsal blood vessel of *Lumbriculus variegatus,* Comp Biochem and Phys 151:467-72

Izhikevich EM (2003) Simple model of spiking neurons. IEEE Trans Neural Netw 14:1569-72.

Johnston JB (1903) On the blood vessels, their valves and the course of the blood in Lumbricus, Biological Bulletin 5:74-84.

Johnston JB, Johnson SW (1902) The course of the blood flow in Lumbricus, American Naturalist 36:317-28.

Koester J, Mayeri E, Liebeswar G, Kandel ER (1973) Cellular regulation of homeostasis: neuronal control of the circulation in Aplysia, Fed Proc 32:2179-87.

Lesiuk NM, Drewes CD (1999a) Blackworms, blood vessel pulsations & drug effects, American Biology Teacher 61:48-53.

Lesiuk N, Drewes CD (1999b) Autotomy reflex in a freshwater oligochaete, *Lumbriculus variegatus* (Clitellata: Lumbriculidae), Hydrobiologia 406:253-261.

Möhl B (1985) The role of proprioception in locust flight control. II. Information signaled by forewing stretch receptors during flight, Journal of Comparative Physiology a-Sensory Neural and Behavioral Physiology 156:103-16.

Müller OF (1774) *Vermivm terrestrium et fluviatilium, seu animalium infusoriorum, helminthicorum, et testaceorum, non marinorum, succincta historia. Volumen alterum,* pp I-XXVI [= 1-36], 1-214, [1-10]. Havniæ & Lipsiæ. (Heineck & Faber).

Parnas I, Abbott BC, Lang F (1969) Electrophysiological properties of Limulus heart and effect of drugs, Am. J Physiol 217:1814-22.

Prosser C, Brown F, Bishop D, Jahn T, Wulff V (1950) Comparative Animal Physiology. Philadelphia, PA: W.B. Saunders Co.

Ŝolc D (2007) The heart and heart conducting system in the kingdom of animals: A comparative approach to its evolution, Exp Clin Cardiol 12:113-18.

Stent GS, Thompson WJ, Calabrese RL (1979) Neural control of heartbeat in the leech and in some other invertebrates, Physiol Rev 59:101-36.

Stephenson J (1930) The Oligochaeta. London: Oxford University Press.

Wenning A, Gennady S, Cymbalyuk GS, Calabrese RL (2004) Heartbeat control in leeches. I. Constriction pattern and neural modulation of blood pressure in intact animals, J Neurophysiol 91:382-96.

Zoran MJ, Martinez CG (2009) *Lumbriculus variegatus* and the Need for speed: A model system for rapid escape, regeneration and asexual reproduction, In: Annelids in Modern Biology (Shain DH, ed), pp 185-202. Hoboken, NJ: John Wiley & Sons, Inc.